Universiteit
Leiden
The Netherlands

Seizures, spreading depolarizations and sudden death

Jansen, N.A.

Citation
Jansen, N. A. (2026, March 11). *Seizures, spreading depolarizations and sudden death*. Retrieved from https://hdl.handle.net/1887/4297304

Version:	Publisher's Version
License:	Licence agreement concerning inclusion of doctoral thesis in the Institutional Repository of the University of Leiden
Downloaded from:	https://hdl.handle.net/1887/4297304

Note: To cite this publication please use the final published version (if applicable).

Part II

Mechanisms of sudden death

Chapter 4

Brainstem spreading depolarization and cortical dynamics during fatal seizures in *Cacna1a*^{S218L} mice

Inge C.M. Loonen*
Nico A. Jansen*
Stuart M. Cain*
Maarten Schenke
Rob A. Voskuyl
Andrew C. Yung
Barry Bohnet
Piotr Kozlowski
Roland D. Thijs
Michel D. Ferrari
Terrance P. Snutch
Arn M.J.M. van den Maagdenberg
Else A. Tolner

*These authors contributed equally

Brain 2019;142(2):412-425

ABSTRACT

Sudden unexpected death in epilepsy (SUDEP) is a fatal complication of epilepsy in which brainstem spreading depolarization may play a pivotal role, as suggested by animal studies. Spatiotemporal details of spreading depolarization occurring in relation to fatal seizures have however not been investigated. In addition, little is known about behavioral and neurophysiological features that may discriminate spontaneous fatal from non-fatal seizures. Transgenic mice carrying the missense mutation S218L in the $\alpha 1_A$ subunit of $Ca_V2.1$ (P/Q-type) Ca^{2+} channels exhibit enhanced excitatory neurotransmission and increased susceptibility to spreading depolarization. Homozygous *Cacna1a*^{S218L} mice show spontaneous non-fatal and fatal seizures, occurring throughout life, resulting in a reduced life expectancy. To identify characteristics of fatal and non-fatal spontaneous seizures, we compared behavioral and electrophysiological seizure dynamics in freely behaving homozygous *Cacna1a*^{S218L} mice. To gain insight in the role of brainstem spreading depolarization in SUDEP, we studied the spatiotemporal distribution of spreading depolarization in the context of seizure-related death. Spontaneous and electrically induced seizures were investigated by video-monitoring and electrophysiological recordings in freely behaving *Cacna1a*^{S218L} and wild-type mice. Homozygous *Cacna1a*^{S218L} mice showed multiple spontaneous tonic-clonic seizures and died from SUDEP in adulthood. Death was preceded by a tonic-clonic seizure terminating with hindlimb clonus, with suppression of cortical neuronal activity during and after the seizure. Induced seizures in freely behaving homozygous *Cacna1a*^{S218L} mice were followed by multiple spreading depolarizations and death. In wild-type or heterozygous *Cacna1a*^{S218L} mice, induced seizures and spreading depolarization were never followed by death. To identify temporal and regional features of seizure-induced spreading depolarization related to fatal outcome, diffusion-weighted MRI was performed in anesthetized homozygous *Cacna1a*^{S218L} and wild-type mice. In homozygous *Cacna1a*^{S218L} mice, appearance of seizure-related spreading depolarization in the brainstem correlated with respiratory arrest that was followed by cardiac arrest and death. Recordings in freely behaving homozygous *Cacna1a*^{S218L} mice confirmed brainstem spreading depolarization during spontaneous fatal seizures. These data underscore the value of the homozygous *Cacna1a*^{S218L} mouse model for identifying discriminative features of fatal compared to non-fatal seizures, and support a key role for cortical neuronal suppression and brainstem spreading depolarization in SUDEP pathophysiology.

INTRODUCTION

Sudden unexpected death in epilepsy (SUDEP) is a tragic and poorly understood complication of epilepsy[1] (Nashef et al., 2012), affecting primarily young adults.[2, 3] Rare recordings in SUDEP cases demonstrated post-ictal generalized EEG suppression (PGES) and respiratory depression prior to death.[4, 5] Risk of SUDEP appears higher in those with poorly controlled tonic-clonic seizures,[6, 7] especially during sleep.[5, 8] In addition, mutations in a subset of ion channel genes have been linked to SUDEP risk.[9-11]

Mechanisms of SUDEP are largely unknown. Homozygous $K_V1.1$ knockout, and heterozygous $Na_V1.1$ knockout mice, as well as mice with a R176Q missense mutation in RyR2 have been proposed as SUDEP models as the mutant mice exhibit seizures followed by cardiorespiratory arrest.[12-15] In these models, evoked cortical seizures were associated with respiratory arrest, followed by spreading depolarization (SD) in the dorsal brainstem and death. Seizure-related hypoxia was proposed as a critical trigger of brainstem SD, resulting in loss of brainstem control over respiration inducing further hypoxia and eventually cardiac arrest.[14]

Transgenic mice carrying the familial hemiplegic migraine type 1 S218L gain-of-function missense mutation in the *Cacna1a* gene, which encodes the α1A subunit of voltage-gated $Ca_V2.1$ (P/Q-type) Ca^{2+} channels,[16] exhibit enhanced excitatory neurotransmitter release and increased susceptibility to induced cortical SD.[16-22] SD can propagate to distinct subcortical regions in homozygous *Cacna1a*^{S218L} mice, but is typically constrained to the cortex in wild-type mice.[20, 22] Patients with the *CACNA1A* gain-of-function S218L mutation suffer from hemiplegic migraine that can be associated with seizures and lethality following minor head trauma.[23-25] Homozygous *Cacna1a*^{S218L} mice display spontaneous seizures and fatal events, that can occur throughout life and have been associated to epileptic attacks.[16]

We here compared behavioral and electrophysiological non-fatal and fatal seizure dynamics in *Cacna1a*^{S218L} mice under freely behaving conditions to assess their value as a SUDEP model and investigate SUDEP mechanisms. We employed diffusion-weighted MRI (DW-MRI) to investigate seizure-related propagation of SD to distinct brain regions in anesthetized mice and studied the incidence of brainstem SD during spontaneous seizures in freely behaving homozygous *Cacna1a*^{S218L} mice.

MATERIALS AND METHODS

Animals

Knock-in *Cacna1a*^{S218L} mice harboring the human missense mutation S218L in the mouse *Cacna1a* gene were generated using a gene-targeting approach.[16] Mice (mutant and wild-type littermates), backcrossed to C57BL/6J for at least 10 generations, of 2.5 to 6.5 months were used. Mutant homozygous *Cacna1a*^{S218L} mice were investigated, except for evoked seizure experiments in freely behaving mice, for which both heterozygous and homozygous *Cacna1a*^{S218L} mice were used. Male mice were used, except for behavioral recordings in naive (non-implanted) mice and DW-MRI experiments under anesthesia, for which both male and female mice were used.

Mice were kept under standard housing conditions with a 12-hour light/dark cycle and food and water ad libitum. Mice freely moving during experiments were housed individually. Experimental procedures were carried out during the light period between 10 a.m. and 5 p.m. Experiments were approved by local ethical committees in accordance with recommendations of the European Communities Council Directive (2010/63/EU) (Leiden) or the Canadian Council for Animal Care guidelines (Vancouver). Experiments were carried out in accordance with ARRIVE guidelines. All efforts were made to minimize animal suffering.

Surgery for electrode placement

Cortical EEG electrodes (single or paired 75 µm platinum (Pt)/iridium (Ir), PT6718; Advent Research Materials) were implanted under isoflurane anesthesia (induction 4%; maintenance 1.5% in oxygen-enriched air) at the following coordinates (mm to bregma): 0.5 anterior/2.0 lateral/0.6 depth (left and right sensorimotor cortex (M1/S1); paired Pt/Ir); 3.5 posterior/2.0 lateral/0.5 depth (right visual cortex (V1); single Pt/Ir); two ball-tip electrodes were placed above the cerebellum and served as reference (Ag) and ground (Ag/AgCl). For cortical stimulation experiments, the left M1/S1 electrodes were implanted at 0.2 mm depth. For ECG recordings, 75 or 150 µm Pt/Ir electrodes were placed subcutaneously over the left latissimus dorsi muscle and the right trapezius and/or latissimus dorsi and tunneled to the skull. For brainstem DC recordings, electrodes were implanted at the following coordinates (mm to bregma): 4.8 posterior/0.8 lateral/3.7 depth (oral pontine reticular nucleus (PnO); single Pt/Ir) and 6.7 posterior/1.3 lateral/3.8 depth (medullary reticular formation (MRF); single Pt/Ir). Electrodes were connected to a 7-channel pedestal (E363/0 socket contacts and MS373 pedestal, Plastics One) and secured to the skull using dental cement (DiaDent Europe). Carprofen (5 mg/kg, s.c.) and Temgesic (0.1 mg/kg, s.c.; only in homozygous *Cacna*^{1aS218L} mice) were administered for post-operative pain relief.

Electrophysiological recordings in freely behaving mice

Wild-type and heterozygous *Cacna1a*^{S218L} mice were allowed to recover for 1 week following surgery (except for a subset of heterozygous *Cacna1a*^{S218L} mice that were studied on the day of surgery). Homozygous Cacna1aS218L mice were given a shorter recovery period of 1 h to minimize

chances of missing fatal seizures, which mostly occurred within 5 days after surgery (see Fig. 1A). Recordings in freely behaving mice were performed as described previously.[26] Electrophysiological signals were 3X pre-amplified and fed into separate direct current (DC) potential (500 Hz low-pass; 10X gain) and alternating current (AC) potential (0.05-500 Hz; 800X gain for electrocorticogram (ECoG); 400X gain for ECG; 200X gain for stimulation experiments) amplifiers. Signals were digitized (Power 1401 and Spike2 software, CED) at 1,000 Hz (DC-potential) or 5,000 Hz (ECoG and ECG). Differential signals from paired cortical electrodes were used to detect multi-unit activity (MUA; 500-5,000 Hz; 12,000-36,000X amplification; 25,000 Hz sampling rate). Video recordings were made using a CCD camera (acA1300-60gmNIR, 30 frames/s, Basler). Locomotor activity was recorded using a custom-built passive infrared motion detection sensor.

Analysis of electrophysiological data

Electrophysiological data were analyzed offline using Spike2 software and custom-written MATLAB scripts (The Mathworks). AC-signals were inspected for electrographic seizures, defined as rhythmic discharges (spikes, sharp waves and/or slow waves) with a duration of > 5 s. For peri-ictal power analyses, AC-signals were artifact-rejected, digitally low-pass filtered (Chebyshev IIR 8th order filter) and down-sampled to 500 Hz. Next, a Fast Fourier Transform was performed using a Hamming window of 4 s. Total power was calculated for different spectral bands: delta (1-5 Hz), theta (5-10 Hz), alpha (10-15 Hz), beta (15-30 Hz), gamma (30-45 Hz) and total (1-100 Hz). SDs (in cortex or brainstem) were detected by the presence of a transient negative DC shift with amplitudes > 5 mV on at least 2 recording locations within 60 s from one another. Terminal depolarization was identified by a prolonged DC-shift without recovery in all channels.

Wave marks were identified from MUA recordings in Spike2 using a detection window of 1 ms to extract the population firing rate. Thresholds were set offline above noise level, defined as overall activity during a 1-min period after the terminal depolarization. Consistency of the MUA signal over the recording period was verified for all recordings by comparison of average firing rates across vigilance states. For comparison across animals, ECoG and MUA data were normalized by the respective activity in a 5-min baseline period of continuous non-rapid eye movement (non-REM) sleep. For ECG analyses, R-peak detection was performed in MATLAB.

Electrically induced seizures in freely behaving mice

In the majority of homozygous *Cacna1a*^{S218L} mice (8/11), seizures were induced on the day of surgery, except for a small separate group of mutant mice (n = 3), in which seizures were induced 2 weeks after surgery (by comparing both groups of homozygous mutants it was assessed whether immediate effects of local tissue damage due to the surgical procedure confounded seizure outcome). In the majority of heterozygous *Cacna1a*^{S218L} mice (7/9) and all wild-type mice (n = 7), seizures were induced 2 weeks after surgery, except for a small separate group of heterozygous *Cacna1a*^{S218L} mice (n = 2) that were stimulated on the day of surgery (for comparison of seizure outcome between heterozygous and homozygous *Cacna1a*^{S218L} mice stimulated on the day of surgery).

Electrical stimulation (15-s train consisting of 1-ms bipolar pulses at a frequency of 8 Hz at incrementally increasing current steps (0.25-4 mA) from a constant-current stimulus isolator (A395, WPI)) was administered every 5 min to determine the threshold for afterdischarges (> 5 s) and/or cortical SD recorded in contralateral M1/S1. For experiments performed 2 weeks after surgery, threshold stimulation was repeated the next day for five times with 20-min intervals. If afterdischarges and/or cortical SDs lasted more than 10 min, no subsequent stimuli were administered. For experiments performed on the day of surgery, stimulation sessions were combined on the first day due to high mortality.

Behavioral analysis

Video recordings of the 24 h preceding a fatal seizure were inspected for seizure-related behavior. Single seizures or seizure clusters lasting more than 30 min were regarded as status epilepticus, which qualifies as an exclusion criterion for SUDEP[1] and were therefore excluded from further analysis. Seizure severity was determined using the Racine-scale[27] with slight adaptation whereby the most severe stage 5 also included jumping circling and wild-running behavior. Subconvulsive stage 1/2 seizures were sporadically observed during video analysis but were not considered for further analysis due to low detection sensitivity and absence of ECoG changes. Convulsive stage 3/4 seizures could reliably be detected from video analysis, and showed similar but milder changes of ECoG as observed for stage 5 seizures. Specific behavioral components during the fatal and last non-fatal seizure occurring at least 1 h before the fatal seizure, were analyzed using software for quantitative behavioral assessment (Observer XT, Noldus Information Technology). Vigilance state was determined by inspection of V1 power spectra and behavioral activity, assessed from video and movement sensor, and categorized as (1) awake (high theta and low delta ECoG activity, during behavioral activity), (2) non-REM sleep (high delta activity, no movements) and (3) REM sleep (high theta and low delta activity following a period of non-REM sleep, no movements).

Naive mice were continuously videotaped. Recordings were assessed for spontaneous seizures in the 24 h preceding a fatal seizure and analyzed as described above.

DW-MRI during induced seizures in anesthetized mice

SD is accompanied by an influx of water to the intracellular compartment of brain cells that causes a decrease in MRI apparent diffusion coefficient.[28] Here, a recently developed DW-MRI protocol that allows SD visualization with high time-resolution[22] was combined with ECoG recordings and cortical electrical stimulation. Animals were anesthetized using isoflurane (2-5% in 100% oxygen) during surgical preparation and once implanted transferred to dexmedetomidine/fentanyl/midazolam and spontaneous breathing of normal air for at least 25 min prior to DW-MRI. Carbon fiber electrodes (WPI) were used, given their compatibility with MRI: two in left M1/S1 for stimulation, one in right M1/S1 for ECoG, and one as reference electrode in the cerebellum (coordinates as described above). MRI experiments were performed on a 7 Tesla animal scanner (Bruker). A quadrature radiofrequency coil with 70-mm inner diameter volume was used for

pulse transmission and the MRI signal was received with a 14-mm diameter actively decoupled surface coil. The mouse was laid supine in the MRI cradle with electrodes fed through the center of the radiofrequency coil. Stimulation electrodes were connected to a constant current unit and stimulator (Grass Technologies) outside the scanner. ECoG electrodes were connected to a W2100 amplifier/receiver outside the scanner (Multichannel Systems) and data was acquired at 0.1-1,000 Hz. Respiratory rate, heart rate and body temperature were monitored during scanning with a Model 1025 Control/Gating system (SA Instruments). DW-MRI was acquired using DW spin-echo planar imaging (EPI) with a b-value of 1800 s/mm^2 (echo time/repetition time = 29/2000 ms, 4 shots, field of view = 2x2 cm, matrix size = 64x64, slice thickness = 1.25 mm, 8 interleaved slices) resulting in an 8-s time resolution.

Electrical stimulation was performed as described above until afterdischarges and/or cortical SDs were observed during 15-min DW-MRI scans. Stimulation was applied at 1, 6 and 11 min with increasing stimulation intensity. If afterdischarges were not observed, a second scan with higher intensity stimulations was performed, and similarly for a third scan, if required (scan set 1 [0.25, 0.5, 1], scan set 2 [2, 4, 8], scan set 3 [10, 15, 20] mA). If the animal survived the threshold voltage, stimulation was reapplied at 20-min intervals for 1 h. Seizures were identified by motion artifacts resulting from clonus during DW-MRI acquisition and epileptiform spiking (2-10 Hz) in the ECoG. DW-MRI data were post-processed in MATLAB and ImageJ software (National Institutes of Health) to mask non-brain structures, apply color maps and measure voxel intensity in defined brain regions.[22] Identification of DW-MRI SD events was defined by an increase in signal intensity exceeding 2X the standard deviation of baseline DW-MRI intensity, sustained for a minimum of 24 s in a single region of interest and visually demonstrating a propagating wave pattern into adjacent structures.

Histology

Following experiments, surviving animals were euthanized by CO_2 and transcardially perfused (0.1 M phosphate-buffered saline followed by 4% paraformaldehyde (PFA) in 0.1 M phosphate buffer). Brains were removed, post-fixed in 4% PFA for 2.5 h at room temperature and sucrose-processed. For mice that died during experiments, brains were post-fixed in 4% PFA for 24 h at 4°C. Brains were sagittally sectioned on a sliding microtome (Leica) and sections (40 µm) were Nissl stained to verify electrode locations.

Statistical Analysis

Data visualization and statistical testing were performed using MATLAB and Graphpad Prism (GraphPad). Unless indicated otherwise, data were presented as mean ± SEM and analyzed using 2-tailed paired or unpaired *t*-tests, Mann-Whitney U test, or repeated measures one-way or two-way ANOVA, where appropriate. A P-value < 0.05 was considered significant.

RESULTS

Homozygous *Cacna1a*^{S218L} mice exhibit hallmark features of SUDEP

We first analyzed the occurrence of spontaneous death in homozygous *Cacna1a*^{S218L} mice (n = 27; all males, age 2.5-5.5 months) with implanted electrodes. Twelve mice died within the 1-h recovery period following surgery, i.e. before the start of electrophysiological recordings. Video-analysis (when available) confirmed death following seizure activity. Of the mice that survived the immediate post-surgical period (n = 15), fatal seizures were observed immediately preceding definitive behavioral arrest and death (n = 13; Fig. 1A). One animal survived the 2-week recording period, and one died following status epilepticus (and was excluded from further analysis).

Chronic electrode implantation may influence seizure characteristics by causing brain damage thus fatal seizure behavior was also studied in non-implanted animals. Among naive (non-implanted) homozygous *Cacna1a*^{S218L} mice with fatal events (n = 11 in 6 males and 5 females); in 8 mice seizure behavior was observed immediately preceding definitive behavioral arrest, similar to the fatal seizure phenotype in implanted mice. In the remaining mice (n = 3), seizure-related behavior was followed by a prolonged period (3-22 h) of immobility before death. In both groups implanted and naive mice, the duration of fatal seizure behavior immediately prior to cessation of motor activity was comparable (Fig. 1B). Most seizures (12/13 in implanted and 7/11 in naive mice) were graded stage 5.[27]

Video inspection of fatal seizures in implanted mice revealed respiratory movements indicative of gasps (between 2 and 5) following behavioral stage 5 seizure activity and preceding terminal depolarization (in 6/12 mice with sufficient quality of video recordings). Concomitant recording of cortical neuronal multi-unit activity (MUA), ECoG (DC- and AC-coupled), and behavior revealed suppression of cortical neuronal activity starting during seizure behavior and continuing up to the terminal depolarization (Fig. 2A). Ictal asystole could be excluded as cause of death in a separate group of mice (n = 5) with cortical and thoracic leads. Electrical cardiac activity was evident minutes after the terminal depolarization (Fig. 2B), with electrocardiographic arrest 315-810 s after terminal depolarization. Periods of ictal bradycardia and atrioventricular block were observed during seizure behavior for all fatal cases, but ventricular fibrillation did not occur until minutes after terminal depolarization.

FIGURE 1. Survival of implanted homozygous *Cacna1a*^{S218L} mice and fatal seizure duration in implanted and naive mice.

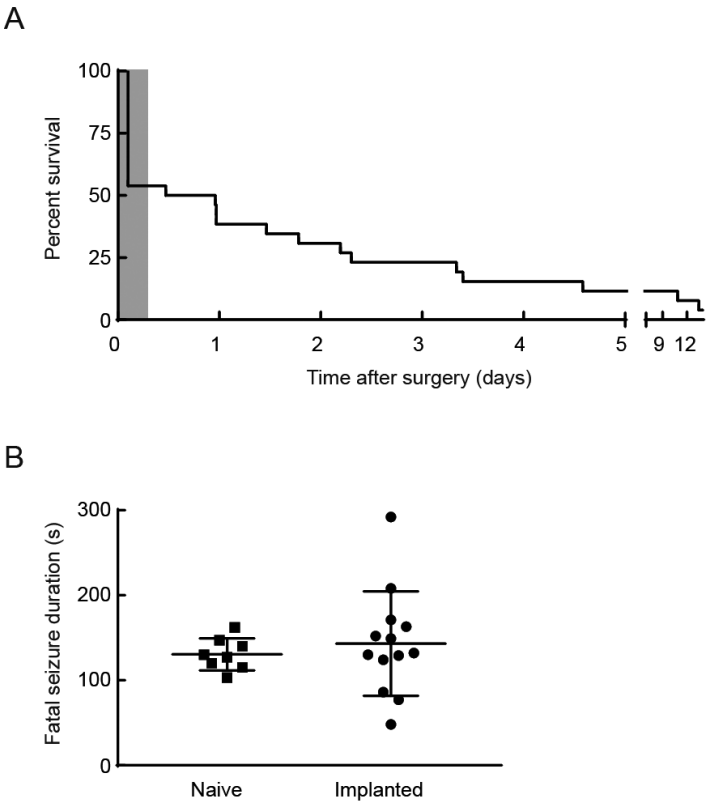

(A) Survival plot of 26 implanted homozygous *Cacna1a*^{S218L} mice showing that the majority of mice died within 1 week after surgery. Note that approximately half (n = 12) died during recovery from surgery (shaded gray), approximately half of the mice (n = 12) died. In the remaining mice (n = 14) that were monitored in the EEG set-up for 2 weeks, fatal seizures occurred in all, except one that survived the recording period. Except for one survivor, all monitored cases (n = 13) showed a fatal seizure preceding death. NB: One case additional mouse died following status epilepticus and was excluded because of death following status epilepticus from further analysis and (not included in the plot). **(B)** Duration of spontaneous fatal seizure behavior was not different for naive and implanted mice (p = 0.50; data shown as mean ± SD).

FIGURE 2. Electrophysiological recordings during spontaneous fatal seizures in homozygous *Cacna1a*^{S218L} mice.

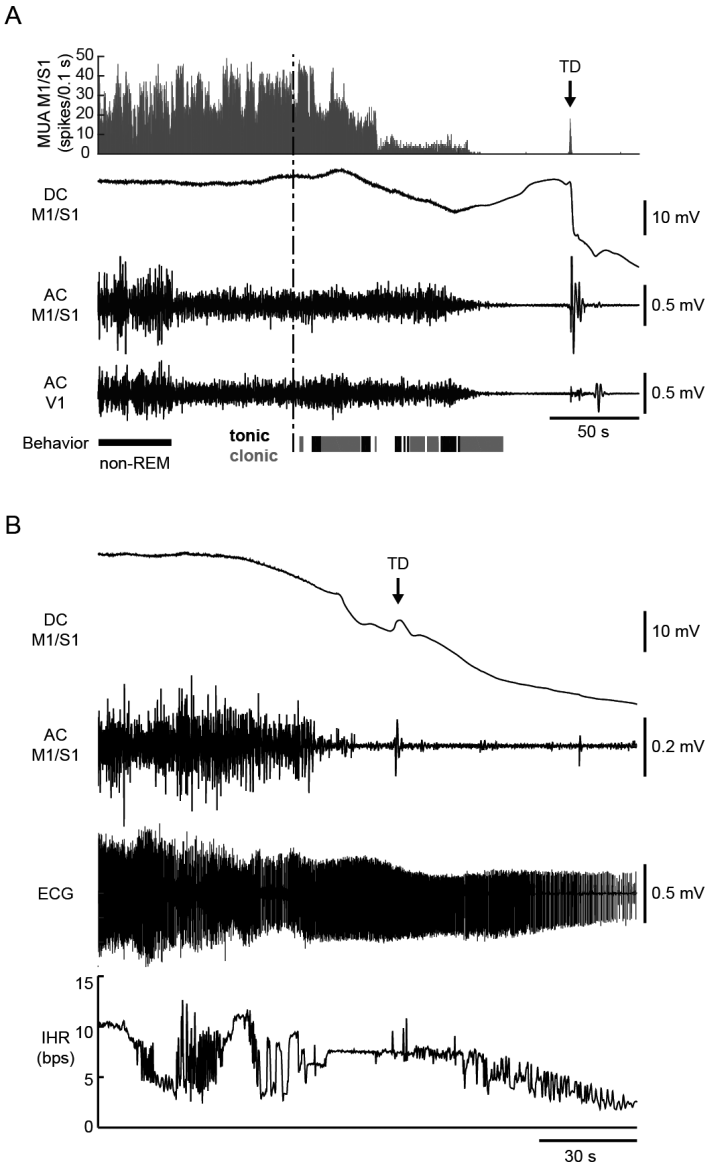

(A) Example of cortical MUA and ECoG (DC and AC) recordings during a fatal seizure (behavioral onset indicated by the vertical dashed line). MUA (histogram) decreased during seizure behavior (clonic behavior in gray, tonic behavior in black). MUA and AC ECoG were attenuated in the minute preceding the terminal depolarization (TD; indicated by an arrow). Note that the pre-ictal transition of AC ECoG amplitude parallels vigilance state (non-REM sleep followed by wakefulness). **(B)** ECG recordings during a fatal seizure in another mouse showing cardiac electrical activity following TD. Electrocardiographic arrest (not shown) occurred 7 min after the TD. The onset of seizure-related behavior preceded the plotted time series. AC = alternating current; Bps = beats per second; DC = direct current; IHR = instantaneous heart rate; REM = rapid eye movement.

Non-fatal and fatal seizures in homozygous *Cacna1a*^{S218L} mice show subtle behavioral differences

To identify discriminative features of fatal seizures, behavioral characteristics were compared between non-fatal and fatal seizures in the 24-h period preceding death in implanted homozygous *Cacna1a*^{S218L} mice. Fatal seizures were typically preceded by multiple behavioral non-fatal seizures (range 1-22/mouse; median 12), of which 41% were classified as stage 3/4 (n = 49 in 9 mice), and 59% as stage 5 (n = 71 in 11 mice). To allow for comparison of non-fatal and fatal seizures independent of seizure severity, only stage 5 seizures were included for further analysis. Non-fatal seizure incidence rates were variable in different animals but seizure frequency did not differ between 0-12 h vs 12-14 h preceding the fatal seizure (p = 0.36; Fig. 3A). Non-fatal seizure duration (averaged per animal) was comparable to fatal seizure duration (191 ± 30 and 131 ± 14 s, respectively; p = 0.37).

Both fatal and non-fatal stage 5 seizures were associated with generalized tonic and clonic behavior and loss of balance, and a subset with circling, jumping and/or wild-running. To detect subtle behavioral differences between the fatal and the last non-fatal seizure (occurring at least 1 h before the fatal seizure), the timing and duration of tonic, clonic, and other seizure behaviors was analyzed in implanted mice (n = 11; Fig. 3B). An increase in clonic behavior was observed in the second half of the fatal seizure. Indeed, closer inspection revealed that all fatal seizures ended with myoclonic jerks of fore- and hindlimbs, gradually decreasing in frequency over a period of 12-36 s. Forelimb clonus always ceased 5-30 s before termination of hindlimb clonus. Non-fatal seizures (n = 11) ended with various seizure-related behaviors (alternating tonic-clonic activity of all limbs (n = 4); exclusive forelimb clonus (n = 4); forelimb and hindlimb clonus (n = 3)). This characteristic pattern of fatal seizure termination, ending with a hindlimb clonus, was also present in naive (non-implanted) *Cacna1a*^{S218L} mice.

The majority of reported human SUDEP events occur at night [5, 8] thus nocturnal patterns in seizure incidence and vigilance state were determined in implanted mice in the 10 min preceding seizures. Stage 5 non-fatal and fatal seizures were equally distributed over the light, dark, and dusk/dawn (transition) phases (Fig. 3C) (non-fatal: 49%, 44% and 7%, respectively; fatal: 50%, 42% and 8%, respectively; p = 0.91). Animals were more often asleep prior to fatal seizures, compared to the last non-fatal seizure, although this difference did not reach statistical significance.

FIGURE 3. Frequency of spontaneous non-fatal and fatal seizures (stage 5) and (pre-)ictal behavior in implanted homozygous *Cacna1a*^{S218L} mice.

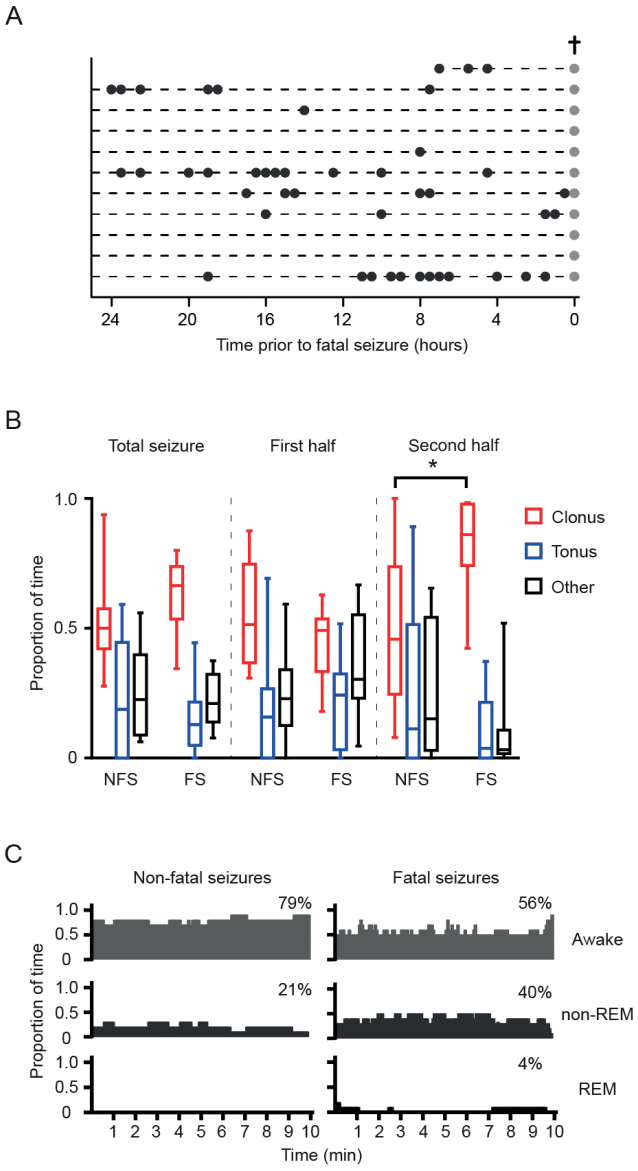

(A) The distribution of non-fatal seizures (black dots) in implanted mice was random over the 24 h preceding the fatal seizure (gray dots; cross). **(B)** Fatal seizures were associated with a proportional increase of clonic behavior during the second half of the seizure at the cost of tonic and other behaviors, when compared to non-fatal seizures ($n = 11$ per group; *$p = 0.001$). **(C)** Vigilance state preceding non-fatal and fatal seizures (percentages indicate fraction of total time) was not significantly different ($p > 0.99$). NFS = non-fatal seizures; FS = fatal seizures; REM = rapid eye movement.

Fatal seizures are associated with specific ECoG dynamics and (post-) ictal neuronal suppression

In implanted homozygous *Cacna1a*^{S218L} mice, rhythmic high-amplitude cortical epileptiform events were never observed during spontaneous non-fatal or fatal seizures (stage 5) but only occurred during status epilepticus (1 non-fatal and 1 fatal). Rather, seizures were associated with reduced ECoG amplitude followed by a period of rhythmic theta band activity (Fig. 4B) and medium-amplitude spikes during pronounced clonic behavior, which often coincided with cortical neuronal suppression (Fig. 4C). Group analysis of (pre)ictal ECoG dynamics confirmed attenuation of total ECoG power, which, for fatal seizures, resulted in complete ECoG suppression during and following the behavioral seizure and never recovered (Fig. 4D). For non-fatal seizures, such suppression of ECoG power was rarely observed (3/54 seizures; example in Supplementary Fig. 1). A decrease in normalized ECoG delta band activity was observed during the first minute of seizure-related behavior for all seizures (Fig. 4E), whereas normalized theta band power was significantly higher during the first minute for fatal compared to non-fatal seizures (Fig. 4F).

Cortical neuronal activity was increased in the seconds to minutes preceding the behavioral onset of the fatal seizure, although not significantly different from non-fatal seizures (Fig. 4G(i) and H). Notably, only during fatal seizures, neuronal activity was significantly attenuated during the last 120 s of seizure-related behavior (Fig 4G(ii) and H). This pattern was followed by low to absent neuronal activity during the post-ictal phase.

Induced seizures in homozygous *Cacna1a*^{S218L} mice are associated with multiple cortical SDs and death

Seizures, induced by stimulation of the sensorimotor cortex, were compared between freely behaving homozygous *Cacna1a*^{S218L} mice (stimulated on the day of surgery (n = 8) or 2 weeks after surgery (n = 3)), heterozygous *Cacna1a*^{S218L} mice (stimulated on the day of surgery (n = 2) or 2 weeks after surgery (n = 7)), and wild-type mice (stimulated 2 weeks after surgery (n = 7)).

Cortical stimulation resulted in severe seizures in all homozygous *Cacna1a*^{S218L} mice (starting immediately to 15.5 min after stimulation) that were fatal in 7 mice. Six mice died following single or multiple stage 5 seizures 2-73 min after stimulation (median 5 min); one mouse died following status epilepticus. Cortical stimulation never resulted in fatal seizures in heterozygous *Cacna1a*^{S218L} mice or wild-type mice. Epileptiform afterdischarges were observed in all heterozygous *Cacna1a*^{S218L} mice and wild-type mice (examples in Fig. 5A and B), but only in 2 out of 11 homozygous *Cacna1a*^{S218L} mice.

Afterdischarges were followed by a single cortical SD, recorded contralateral to the stimulation electrode, in all but one heterozygous *Cacna1a*^{S218L} mice whereas no cortical SDs were observed in wild-type mice (examples in Fig. 5A and B). Severe seizure behavior in homozygous *Cacna1a*^{S218L} mice was, however, associated with multiple cortical SDs (n = 2-38 waves, median 21, in 9/11 mice; example in Fig. 5C). These findings indicate that fatal seizure outcome in homozygous *Cacna1a*^{S218L} mice may relate to an enhanced propensity to seizure-associated SD.

FIGURE 4A-4C. Different ECoG and cortical multi-unit activity during spontaneous non-fatal and fatal seizures in homozygous *Cacna1a*^{S218L} mice.

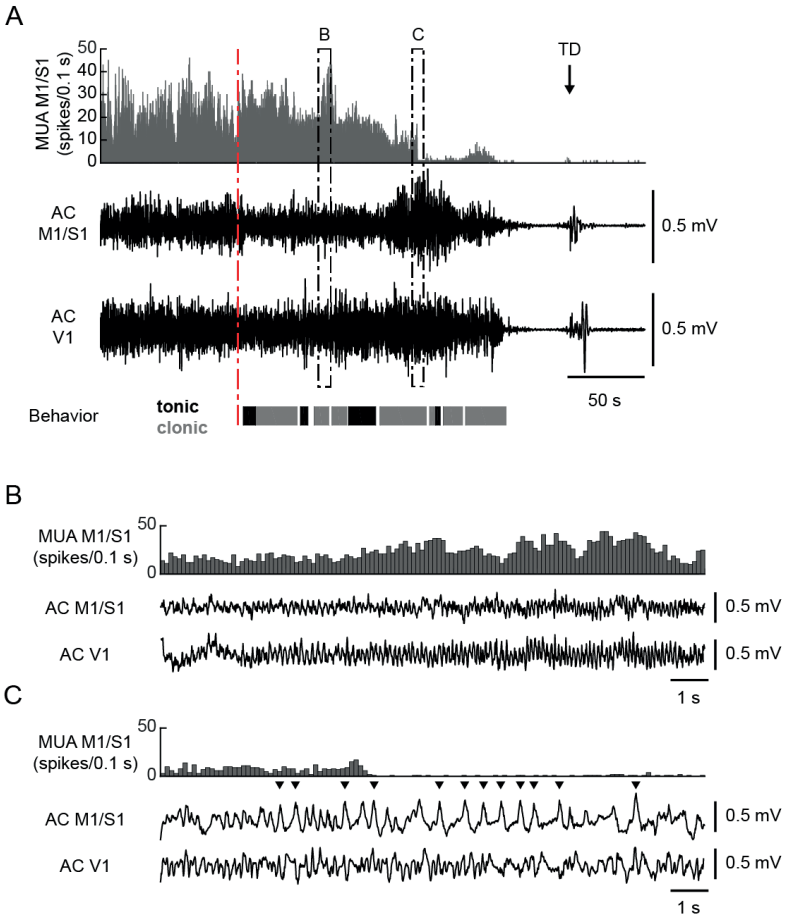

(A) Example cortical MUA and AC ECoG recordings of a fatal seizure (behavioral onset indicated by a red dashed line; clonic behavior is shown in gray, tonic behavior in black; terminal depolarization (TD) indicated by an arrow). Details of ictal AC ECoG and MUA indicated by dashed boxes are shown in panels B and C. **(B)** Detailed inspection of the AC ECoG reveals oscillatory activity corresponding to theta band frequencies and **(C)** spike-wave complexes (indicated by arrowheads) not exceeding normal AC ECoG amplitude, that coincide with loss of cortical MUA.

FIGURE 4D-4H. Different ECoG and cortical multi-unit activity during spontaneous non-fatal and fatal seizures in homozygous *Cacna1a*^{S218L} mice.

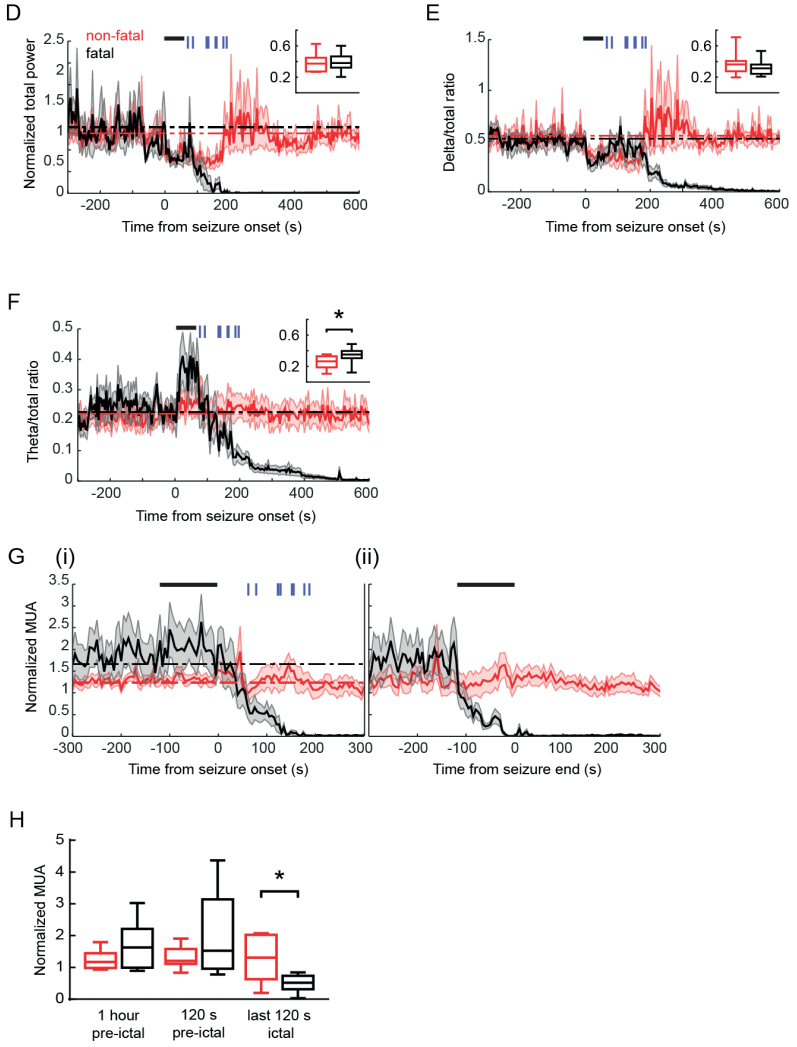

(D, E, F) Spectral analyses of primary sensorimotor (M1/S1) AC ECoG during non-fatal (red) and fatal (black) stage 5 seizures ($n = 9$) for total power **(D)**, delta/total ratio **(E)** and theta/total ratio **(F)**. Power during the first 60 s of all seizures (indicated by black bars) was compared with baseline power (1 h pre-ictal; baseline power levels for non-fatal/fatal seizures are indicated by red/black dashed lines). In addition, non-fatal and fatal seizures were compared over the same ictal period (insets; data is shown as mean ± SD). Normalized total power and delta/total power ratio were attenuated (D and E; $p = 0.001$ and $p = 0.010$ for non-fatal and fatal seizures, respectively). Theta/total ratio was increased only for fatal seizures, compared to both baseline and non-fatal seizures (F; $p < 0.001$ and $^*p = 0.003$, respectively). For all fatal seizures, cessation of seizure-related behavior is indicated by vertical blue bars. **(G, H)** Normalized cortical MUA dynamics in relation to onset **(G(i))** and end **(G(ii))** of seizure-related behavior. Black bars indicate 120-s time windows used for comparison of non-fatal and fatal seizures in (H). MUA decreased during fatal seizures **(G)** and was significantly reduced when compared to non-fatal seizures during the last 120 s of seizure-related behavior (**H**; $^*p = 0.018$). AC = alternating current.

FIGURE 5. Multiple cortical spreading depolarizations associated with induced seizures followed by death in homozygous *Cacna1a*^{S218L} mice.

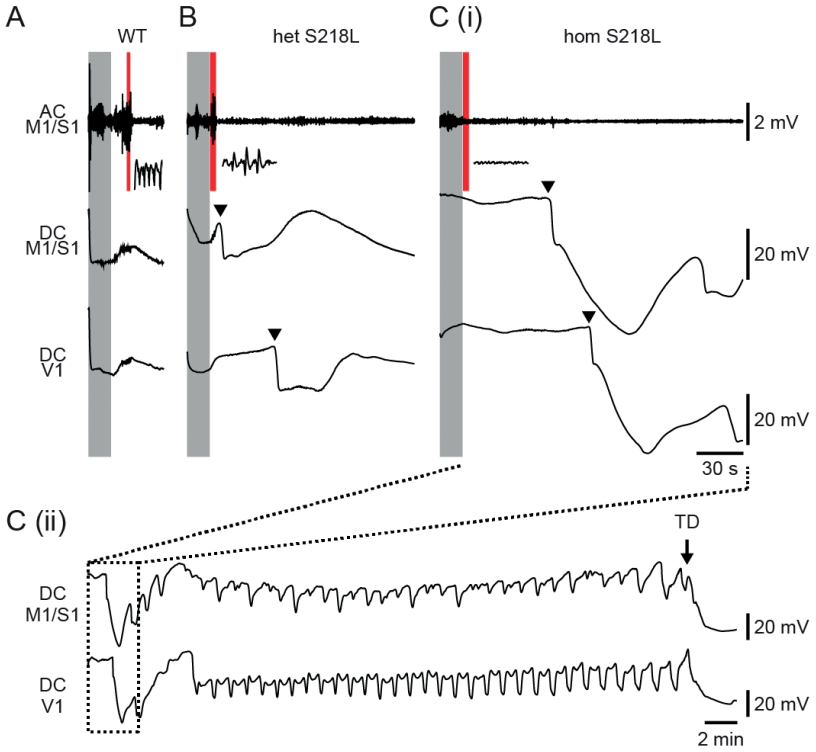

Representative ECoG (AC and DC) recordings showing that stimulation (shaded gray) was followed by afterdischarges in all wild-type (WT) mice (7/7; example in **(A)**) as indicated by insets (corresponding to the shaded red time windows) and heterozygous *Cacna1a*^{S218L} (het S218L) mice (9/9; example in **(B)**), while only in a minority of homozygous *Cacna1a*^{S218L} (hom S218L) mice (2/11; example in **(C(i)B)**, as indicated by insets (corresponding to the shaded red time windows). Cortical SD (indicated by arrowheads in example traces) was observed directly following afterdischarges in all but one heterozygous *Cacna1a*^{S218L} mice. In the homozygous *Cacna1a*^{S218L} mice multiple cortical SDs occurred, followed by a terminal depolarization **(C(ii)B(ii)**; TD; indicated by an arrow). Fatal outcome was observed in 7 out of 11 homozygous *Cacna1a*^{S218L} mice but none of the wild-type and heterozygous *Cacna1a*^{S218L} mice. AC = alternating current; DC = direct current.

Induced fatal seizures in homozygous *Cacna1a*^{S218L} mice are associated with brainstem SD

DW-MRI was used to assess the spatiotemporal propagation of SDs in response to cortically induced seizures in anesthetized homozygous *Cacna1a*^{S218L} (n = 7) and wild-type (n = 3) mice. SD occurrence, visualized by MRI-diffusional changes associated with SD-related cell swelling, was confirmed by simultaneous (ipsilateral) cortical DC recording (Supplementary Fig. 2). Stimulation resulted in epileptiform afterdischarges (2-10 Hz), concurrent with DW-MRI movement artifacts directly following stimulation. In wild-type mice stimulation resulted only in non-fatal seizures (n = 10), while in homozygous *Cacna1a*^{S218L} mice both non-fatal seizures (n = 15) and fatal seizures (n = 4) were observed.

DW-MRI data (from the hemisphere ipsilateral to the stimulation site) showed cortical SD with all fatal (4/4) and most non-fatal seizures (13/15) in homozygous *Cacna1a*^{S218L} mice and with most non-fatal seizures (7/10) in wild-type mice. Cortical SDs were first observed in the dorsal sensorimotor cortex and propagated to the visual cortex with different timing delays between genotypes (in s): wild-type: 43 ± 6; *Cacna1a*^{S218L} non-fatal: 26 ± 3; *Cacna1a*^{S218L} fatal: 20 ± 2 (wild-type vs *Cacna1a*^{S218L} non-fatal: p = 0.016; wild-type vs *Cacna1a*^{S218L} fatal: p = 0.018; *Cacna1a*^{S218L} non-fatal vs *Cacna1a*^{S218L} fatal: p = 0.72). For fatal seizures, cortical SDs were followed by SDs in subcortical structures including striatum (14 ± 13 s, indicating the time delay following SD in the sensorimotor cortex), hippocampus (16 ± 1 s), superior and inferior colliculus (24 ± 5 s) and brainstem (31 ± 4 s) (Fig. 6A, B and E). Within the brainstem, SD in the medulla was detected after SD appearance in the pons (3/4 fatal seizures; delay of 1-3 scan repetitions; 8-24 s). In one animal medullary and pontine SD were detected at the same time point. For non-fatal seizures in homozygous *Cacna1a*^{S218L} mice, cortical SDs were followed by SDs in striatum (n = 8; 59 ± 11 s), hippocampus (n = 6; 46 ± 10 s), and colliculi (n = 5; 45 ± 13 s), but never in the brainstem (Figs. 6C and E). In all but one wild-type mice, SD was not observed in subcortical structures (Fig. 6D). Cortical SD occurrence in the contralateral cortex was only rarely observed in the DW-MRI experiments following non-fatal seizures (2/10) in wild-type mice, in line with ECoG from freely behaving wild-type mice in which contralateral cortical SD was not observed following stimulation. In summary, subcortical SD propagation is more extensive in homozygous *Cacna1a*^{S218L} mice with brainstem SD only observed during fatal seizures.

Respiratory rate and heart rate, monitored during evoked seizure experiments, were increased after non-fatal seizures in homozygous *Cacna1a*^{S218L} and wild-type mice (Fig. 7). Both parameters returned to baseline within 1 minute in wild-type mice, whereas in homozygous *Cacna1a*^{S218L} mice respiratory rate fluctuated for an extended period of time (2-3 min) before returning to baseline. In fatal seizures, respiratory slowing was followed by respiratory arrest that preceded cardiac arrest. Respiratory arrest occurred near-concurrently with the observation of SD in the brainstem (example in Fig. 7A), either shortly before (12 and 5 s) or after (11 or 33 s) brainstem SD (recognizing that the time resolution of DW-MRI was limited to 8 s).

FIGURE 6A-6D. DW-MRI visualization of spreading depolarization following induced seizures in anesthetized homozygous *Cacna1a*^{S218L} mice.

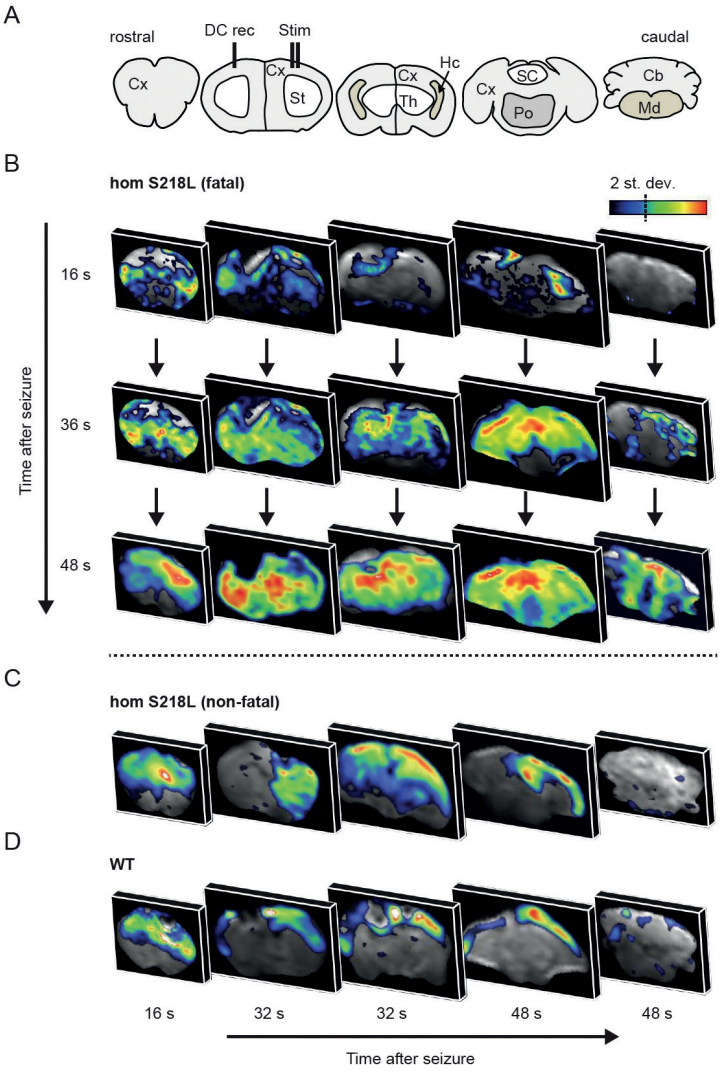

(A) Coronal brain maps corresponding to DW-MRI images in **(B)**, **(C)**, and **(D)**. **(B)** Representative DW-MRI data following an induced fatal and **(C)** non-fatal seizure in a homozygous *Cacna1a*^{S218L} (hom S218L) mouse, and **(D)** a non-fatal seizure in a wild-type (WT) mouse. Data are shown for a single representative time point in each slice, capturing a snapshot of spreading depolarization (SD). Note that in (B) all coronal maps are shown at 3 time points to demonstrate spatiotemporal propagation of SD, whereas in **(C)** and **(D)** different sections at 3 time points are depicted to show the limited subcortical spread of SD in non-fatal seizures.

FIGURE 6E. DW-MRI visualization of spreading depolarization following induced seizures in anesthetized homozygous *Cacna1a*^{S218L} mice.

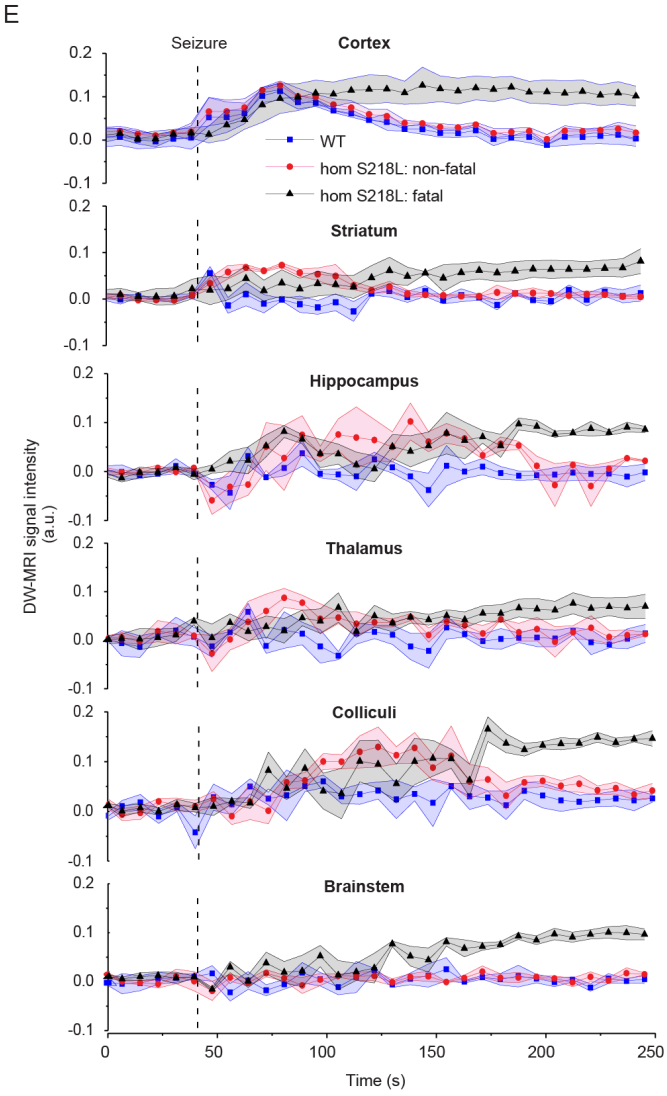

(E) Time course data of wild-type mice (n = 3; 7 SDs) and *Cacna1a*^{S218L} mice (n = 7; 13 non-fatal SDs; 4 fatal SDs) in relation to seizure onset (dashed line) are shown for distinct brain regions obtained from DW-MRI data. In *Cacna1a*^{S218L} mice, SD appeared in the brainstem only during fatal seizures and was constrained to striatum, amygdala, hippocampus and colliculi during non-fatal seizures. Cortical SD occurred in all wild-type and *Cacna1a*^{S218L} mice. A.u. = arbitrary units; Cb = cerebellum; Cx = cortex; DC = direct current; Hc = hippocampus; Md = medulla oblongata; Po = pons; SC = superior colliculus; St = striatum; Th = thalamus.

FIGURE 7. Physiological function following induced seizures during DW-MRI in anesthetized homozygous *Cacna1a*^{S218L} mice.

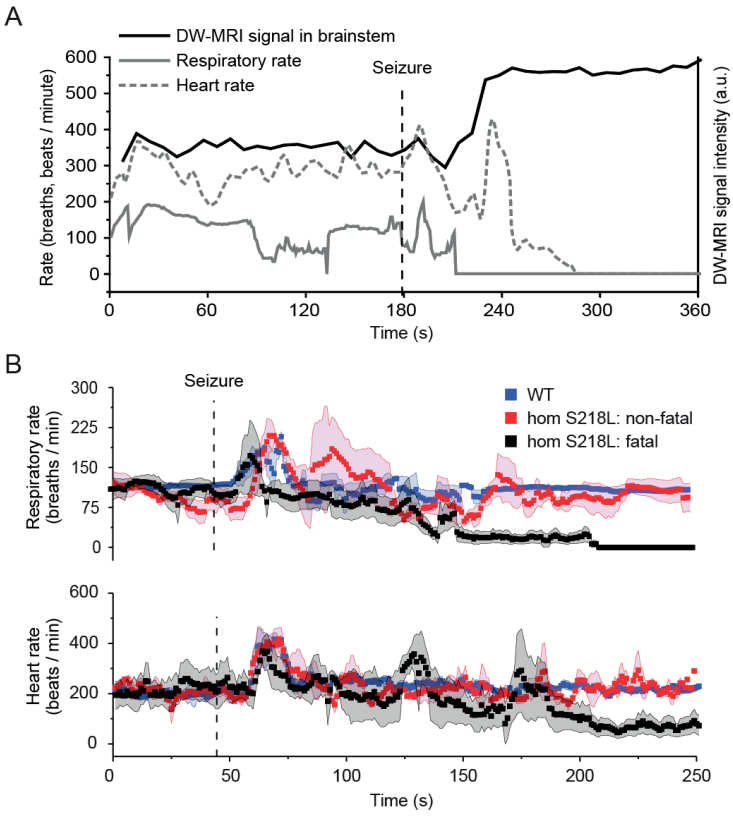

(A) Representative example from a single animal of respiratory rate, heart rate and SD aligned temporally in relation to seizure onset (dashed line). **(B)** Physiological parameters (aligned with SD dynamics shown in Fig. 6E) from homozygous *Cacna1a*^{S218L} (hom S218L) mice, following non-fatal (n = 10) and fatal seizures (n = 4), and wild-type (WT) mice, following non-fatal seizures (n = 15). Simultaneous respiratory (upper trace) and heart rate (lower trace) data acquired during seizures from the same animals showing that, for fatal seizures, respiratory rate decreased until complete arrest and preceded cardiac arrest. A.u. = arbitrary units. Data shown as mean ± SD.

As the amygdala has been implicated in seizure-related respiratory arrest,[29] one could argue that respiratory arrest might be caused by SD occurring in the amygdala. Although SD in the amygdala was observed following cortical SD in *Cacna1a*^{S218L} mice (n = 13) and in wild-type mice (n = 2), this did not coincide with profound respiratory changes (Supplementary Fig. 3).

Brainstem SD occurs during spontaneous fatal seizures in homozygous *Cacna1a*^{S218L} mice

To study the incidence of brainstem SD during spontaneous seizures in homozygous *Cacna1a*^{S218L} mice, brainstem DC ECoG recordings from the pons (PnO) and medulla (MRF) were combined with V1 ECoG and ECG in freely behaving mice. Three mice had a fatal seizure (duration 185-270 s) - after a recording period of 1-3.5 days - that was always associated with brainstem SD. Brainstem SD had an onset during seizure behavior (24-60 s preceding seizure termination) and was followed by ECoG suppression, bradycardia and a cortical terminal depolarization (example in Fig. 8). Gasping was absent during fatal seizures. A delay in MRF SD was observed in 2 mice (9 and 23 s after PnO SD), whereas in 1 mouse SD occurred simultaneously in PnO and MRF. Brainstem SD was not observed during non-fatal seizures (n = 8) or during interictal recordings preceding the fatal seizure.

FIGURE 8. Brainstem DC recordings during a spontaneous fatal seizure in a homozygous *Cacna1a*^{S218L} mouse.

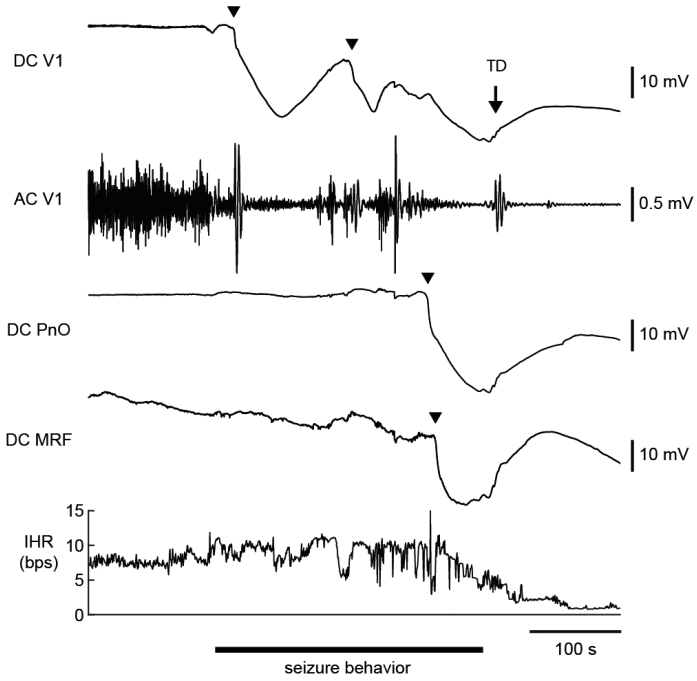

Example of an SD (indicated by arrowheads) that occurred during seizure behavior in the oral pontine reticular nucleus (PnO) and subsequently in the medullary reticular formation (MRF), followed by visual cortex (V1) AC ECoG suppression, bradycardia and cortical terminal depolarization (TD; indicated by an arrow). Note that ictal V1 AC ECoG amplitude was greatly reduced following cortical SD. AC = alternating current; bps = beats per second; DC = direct current; IHR = instantaneous heart rate.

DISCUSSION

Here we describe features that discriminate spontaneous and induced fatal seizures from non-fatal events in homozygous *Cacna1a*^{S218L} mice. Characteristics specific to fatal seizures included: i) an increase in clonic activity during later phases of the seizure, ii) early (ictal) and post-ictal suppression of cortical neuronal activity, iii) subcortical SD spread following induced seizures culminating in brainstem SD with respiratory arrest, and eventually cardiac arrest, and iv) brainstem SD during spontaneous seizures preceding complete ECoG suppression and cardiac arrest.

DW-MRI revealed that cortically-induced non-fatal seizures were associated with SD that remained predominantly restricted to the ipsilateral cortex in wild-type mice, but invaded subcortical structures in *Cacna1a*^{S218L} mice. This is in agreement with previous findings in homozygous *Cacna1a*^{S218L} mice wherein induced cortical SD was followed by striatal and hippocampal[22] and, occasionally, thalamic invasion.[20] Simultaneous cortical DC recordings in a subset of DW-MRI experiments confirm that measured changes in signal intensity indeed result from cortical SD events.

The results from both induced and spontaneous seizures in *Cacna1a*^{S218L} mice indicate that only fatal seizures were associated with brainstem SD, observed in the pons and medulla. This coincided with a decrease in respiratory activity during fatal seizures, suggesting that brainstem SD induces apnea. Although we were unable to measure ictal respiratory activity systematically in freely behaving mice, few post-ictal respiratory gasps were observed in half of the mice whereas in the other half no respiratory activity was observed, indicating limited autoresuscitation. This supports the hypothesis that seizure-induced SD causes death by suppression of brainstem respiratory control. Indeed, in animals with confirmed brainstem SD during the fatal seizure no gasps were observed. Our data contrast with previous studies, where apnea clearly *preceded* brainstem SD, and hypoxia was proposed as a trigger for brainstem SD.[14, 15] Differences in timing between respiratory changes and SD might be explained by methodology, since previous studies relied on electrodes inserted in the dorsocaudal medulla only.[14, 15] Future studies should indicate whether brainstem SD indeed precedes and causes respiratory arrest.

Head trauma due to electrode implantation is likely to have influenced the features of spontaneous fatal seizures in recorded homozygous *Cacna1a*^{S218L} mice. Whereas surgery contributed to seizure frequency and caused a reduction of life span in homozygous *Cacna1a*^{S218L} mice, spontaneous seizure behavior was similar in naive and implanted animals. In addition, cortical stimulation experiments on the day of surgery and after a 2-week recovery period both resulted in fatal seizures in the majority of homozygous *Cacna1a*^{S218L} mice, indicating that acute post-surgery complications are not key contributors to fatal seizure outcome in our model.

All fatal seizures and only a minority of non-fatal seizures in freely behaving *Cacna1a*^{S218L} mice were associated with a late ictal and post-ictal cortical suppression pattern that resembles PGES, a consistent observation in clinical SUDEP recordings.[4, 5] Global[30] and/or local[31] hypoxia could underlie the suppression of cortical neuronal activity. Indeed, in fatal seizures in a mouse

model of Dravet syndrome, an epileptic encephalopathy associated with high SUDEP risk,[11] apnea preceded PGES.[32] Periods of apnea and bradycardia followed by a terminal apnea and asystole have been reported in human SUDEP cases.[5] Our ECG recordings during spontaneous and induced fatal seizures showed intermittent bradycardia. This may indicate autonomic disturbances due to brainstem hyperexcitability, SD, and/or direct effects of intermittent hypoxia on cardiac function and warrants further investigation.

In anesthetized mice in the DW-MRI study fatal outcome occurred within minutes following stimulation whereas in freely behaving mice the delay showed high variation with particularly long delays in some animals. This discrepancy may be explained by consequences of anesthesia, resulting in a reduced respiratory drive in anesthetized animals[33] and possible transient hypoxia that can affect seizure and SD threshold.[34] In freely behaving mice, occurrence of cortical SD following induced seizures will limit spread of seizure activity. With an expected lower cortical SD susceptibility under anesthesia,[35] electrical seizure induction during the DW-MRI experiments may have involved a more extensive seizure network including brainstem areas. Since brainstem SD precedes cortical SD during severe hypoxia,[36] mild hypoxic conditions in anesthetized mice may have increased SD risk in brainstem areas. The short delay between SDs in cortical and subcortical structures in the DW-MRI study would be in line with a contribution of local hyperexcitability, as recent evidence has shown that brainstem epileptiform activity can occur concurrently with fatal seizures.[37] Future studies of fatal seizures in this and other SUDEP mouse models are required to confirm the path of SD propagation from subcortical structures to the brainstem, as suggested by our DW-MRI studies in anesthetized *Cacna1a*^{S218L} mice.

We present *Cacna1a*^{S218L} mice as a relevant and validated model for SUDEP since: (i) homozygous *Cacna1a*^{S218L} mice displayed both non-fatal and fatal seizures, allowing for identification of SUDEP-related seizure dynamics of potential clinical value for anticipating and preventing SUDEP; (ii) mice displayed fatal seizures at various ages reflecting clinical reports of SUDEP incidence rates.[2, 3] A fatal seizure outcome did not occur in heterozygous *Cacna1a*^{S218L} or wild-type mice. Electrographically, cortical epileptiform activity was limited to incidental low-amplitude spikes during myoclonic behavior. This contrasts the pronounced epileptiform activity seen in e.g. $K_V1.1$ and $Na_V1.1$ SUDEP mouse models.[12, 38] However, human semiological, EEG and ECoG data indicate heterogeneity of SUDEP phenomena that involve absence of epileptiform activity and include observations suggesting brainstem involvement.[2, 6, 39] Multiple mechanisms may therefore contribute to SUDEP, and it is conceivable that mechanisms may differ between patients. Clinical reports of monitored SUDEP cases indicated that most fatal events are preceded by tonic-clonic seizures, while in a minority there is no preceding seizure.[5, 40, 41] For those cases in which death was not preceded by epileptiform activity, a brainstem mechanism seems plausible.[40, 41] Practical constraints limit electrography of brainstem areas in human epilepsy. Nevertheless, increased blood flow in the cerebellum, thalamus, and midbrain observed during and following seizure spread in patients with epilepsy supports brainstem involvement in tonic-clonic seizures.[42] Clinical observations also support a link between SUDEP risk and brainstem involvement. Convulsive seizures with tonic

arm extension, thought to coincide with spread of activity to the brainstem, were found to be strongly associated with PGES[30] that is associated with increased SUDEP risk.

Stage 5 seizures generally showed attenuation of the ECoG, with a relative dominance of theta band activity during fatal seizures. ECoG attenuation during seizures has also been reported for idiopathic generalized epilepsy during the tonic phase.[43] The seizure-related behavior in *Cacna1a*^{S218L} mice appears similar to that described for audiogenic seizures in Genetic Epilepsy-Prone Rats (GEPRs), in which ECoG attenuation was observed during tonic hindlimb extension.[44, 45] Behavioral similarities include wild-running, jumping, tonic, and clonic behaviors, which for GEPR models have been linked to involvement of the brainstem reticular formation.[46] Brainstem networks are sufficient for the expression of running and tonic seizure components, whereas generalized clonic seizures require forebrain circuitry.[47, 48] The observed behavioral and ECoG characteristics in *Cacna1a*^{S218L} mice thereby support an important role for the brainstem in the seizure mechanism. We hypothesize that an intricate balance exists between epileptiform activity and SD in *Cacna1a*^{S218L} mice, as indicated by the frequent absence of afterdischarges following cortical stimulation, that may differ for different brain regions and induce seizure activity in brainstem networks while suppressing forebrain seizure activity. Fatal seizures in *Cacna1a*^{S218L} mice specifically terminated with clonic behavior. As brainstem seizure activity may suppress clonic seizure behavior related to the forebrain,[49] the clonic behavior during the second part of fatal seizures in *Cacna1a*^{S218L} mice may result from suppression of brainstem networks by SD. To the best of our knowledge, extensive semiological descriptions of fatal seizures in SUDEP cases that include detailed EEG analyses and timings of tonic and clonic activity are lacking. It therefore remains to be determined whether early cortical neuronal suppression, theta band activity and clonic activity are specific for spontaneous fatal seizures in the *Cacna1a*^{S218L} model or represent a hallmark of SUDEP.

In conclusion, *Cacna1a*^{S218L} mice appear a valid model to study SUDEP mechanisms. Behavioral, neurophysiological and imaging data revealed characteristics specific to fatal seizures, implicating a role for cortical neuronal suppression and brainstem SD in SUDEP pathophysiology. This adds to the fundamental understanding of the processes that underlie seizure termination and risk for SUDEP, and may aid identification of predictive SUDEP biomarkers.

Acknowledgements

The authors thank Mr. Ludo Broos and Dr. Thijs Houben for assistance with histology and electrophysiology.

REFERENCES

1. Nashef, L., et al., Unifying the definitions of sudden unexpected death in epilepsy. *Epilepsia*, 2012. 53(2): p. 227-33.
2. Massey, C.A., et al., Mechanisms of sudden unexpected death in epilepsy: the pathway to prevention. *Nat Rev Neurol*, 2014. 10(5): p. 271-82.
3. Harden, C., et al., Practice guideline summary: Sudden unexpected death in epilepsy incidence rates and risk factors: Report of the Guideline Development, Dissemination, and Implementation Subcommittee of the American Academy of Neurology and the American Epilepsy Society. *Neurology*, 2017. 88(17): p. 1674-1680.
4. Lhatoo, S.D., et al., An electroclinical case-control study of sudden unexpected death in epilepsy. *Ann Neurol*, 2010. 68(6): p. 787-96.
5. Ryvlin, P., et al., Incidence and mechanisms of cardiorespiratory arrests in epilepsy monitoring units (MORTEMUS): a retrospective study. *Lancet Neurol*, 2013. 12(10): p. 966-77.
6. Surges, R., et al., Sudden unexpected death in epilepsy: risk factors and potential pathomechanisms. *Nat Rev Neurol*, 2009. 5(9): p. 492-504.
7. Hesdorffer, D.C., et al., Combined analysis of risk factors for SUDEP. *Epilepsia*, 2011. 52(6): p. 1150-9.
8. Lamberts, R.J., et al., Sudden unexpected death in epilepsy: people with nocturnal seizures may be at highest risk. *Epilepsia*, 2012. 53(2): p. 253-7.
9. Goldman, A.M., et al., Arrhythmia in heart and brain: KCNQ1 mutations link epilepsy and sudden unexplained death. *Sci Transl Med*, 2009. 1(2): p. 2ra6.
10. Bagnall, R.D., et al., Exome-based analysis of cardiac arrhythmia, respiratory control, and epilepsy genes in sudden unexpected death in epilepsy. *Ann Neurol*, 2016. 79(4): p. 522-34.
11. Shmuely, S., et al., Mortality in Dravet syndrome: A review. *Epilepsy Behav*, 2016. 64(Pt A): p. 69-74.
12. Glasscock, E., et al., Kv1.1 potassium channel deficiency reveals brain-driven cardiac dysfunction as a candidate mechanism for sudden unexplained death in epilepsy. *J Neurosci*, 2010. 30(15): p. 5167-75.
13. Moore, B.M., et al., The Kv1.1 null mouse, a model of sudden unexpected death in epilepsy (SUDEP). *Epilepsia*, 2014. 55(11): p. 1808-16.
14. Aiba, I. and J.L. Noebels, Spreading depolarization in the brainstem mediates sudden cardiorespiratory arrest in mouse SUDEP models. *Sci Transl Med*, 2015. 7(282): p. 282ra46.
15. Aiba, I., X.H. Wehrens, and J.L. Noebels, Leaky RyR2 channels unleash a brainstem spreading depolarization mechanism of sudden cardiac death. *Proc Natl Acad Sci U S A*, 2016. 113(33): p. E4895-903.
16. van den Maagdenberg, A.M., et al., High cortical spreading depression susceptibility and migraine-associated symptoms in Ca(v)2.1 S218L mice. *Ann Neurol*, 2010. 67(1): p. 85-98.
17. van den Maagdenberg, A.M., et al., A Cacna1a knockin migraine mouse model with increased susceptibility to cortical spreading depression. *Neuron*, 2004. 41(5): p. 701-10.
18. Eikermann-Haerter, K., et al., Androgenic suppression of spreading depression in familial hemiplegic migraine type 1 mutant mice. *Ann Neurol*, 2009. 66(4): p. 564-8.

19. Tottene, A., et al., Enhanced excitatory transmission at cortical synapses as the basis for facilitated spreading depression in Ca(v)2.1 knockin migraine mice. *Neuron*, 2009. 61(5): p. 762-73.
20. Eikermann-Haerter, K., et al., Enhanced subcortical spreading depression in familial hemiplegic migraine type 1 mutant mice. *J Neurosci*, 2011. 31(15): p. 5755-63.
21. Vecchia, D., et al., Abnormal cortical synaptic transmission in CaV2.1 knockin mice with the S218L missense mutation which causes a severe familial hemiplegic migraine syndrome in humans. *Front Cell Neurosci*, 2015. 9: p. 8.
22. Cain, S.M., et al., In vivo imaging reveals that pregabalin inhibits cortical spreading depression and propagation to subcortical brain structures. *Proc Natl Acad Sci U S A*, 2017. 114(9): p. 2401-2406.
23. Ophoff, R.A., et al., Familial hemiplegic migraine and episodic ataxia type-2 are caused by mutations in the Ca2+ channel gene CACNL1A4. *Cell*, 1996. 87(3): p. 543-52.
24. Kors, E.E., et al., Delayed cerebral edema and fatal coma after minor head trauma: role of the CACNA1A calcium channel subunit gene and relationship with familial hemiplegic migraine. *Ann Neurol*, 2001. 49(6): p. 753-60.
25. Stam, A.H., et al., Early seizures and cerebral oedema after trivial head trauma associated with the CACNA1A S218L mutation. *J Neurol Neurosurg Psychiatry*, 2009. 80(10): p. 1125-9.
26. Houben, T., et al., Optogenetic induction of cortical spreading depression in anesthetized and freely behaving mice. *J Cereb Blood Flow Metab*, 2017. 37(5): p. 1641-1655.
27. Racine, R.J., Modification of seizure activity by electrical stimulation. II. Motor seizure. *Electroencephalogr Clin Neurophysiol*, 1972. 32(3): p. 281-94.
28. de Crespigny, A., et al., Magnetic resonance imaging assessment of cerebral hemodynamics during spreading depression in rats. *J Cereb Blood Flow Metab*, 1998. 18(9): p. 1008-17.
29. Dlouhy, B.J., et al., Breathing Inhibited When Seizures Spread to the Amygdala and upon Amygdala Stimulation. *J Neurosci*, 2015. 35(28): p. 10281-9.
30. Alexandre, V., et al., Risk factors of postictal generalized EEG suppression in generalized convulsive seizures. *Neurology*, 2015. 85(18): p. 1598-603.
31. Farrell, J.S., et al., Postictal behavioural impairments are due to a severe prolonged hypoperfusion/hypoxia event that is COX-2 dependent. *Elife*, 2016. 5.
32. Kim, Y., et al., Severe peri-ictal respiratory dysfunction is common in Dravet syndrome. *J Clin Invest*, 2018. 128(3): p. 1141-1153.
33. Tremoleda, J.L., A. Kerton, and W. Gsell, Anaesthesia and physiological monitoring during in vivo imaging of laboratory rodents: considerations on experimental outcomes and animal welfare. *EJNMMI Res*, 2012. 2(1): p. 44.
34. Wei, Y., G. Ullah, and S.J. Schiff, Unification of neuronal spikes, seizures, and spreading depression. *J Neurosci*, 2014. 34(35): p. 11733-43.
35. Kudo, C., et al., Anesthetic effects on susceptibility to cortical spreading depression. *Neuropharmacology*, 2013. 67: p. 32-6.
36. Richter, F., et al., The relationship between sudden severe hypoxia and ischemia-associated spreading depolarization in adult rat brainstem in vivo. *Exp Neurol*, 2010. 224(1): p. 146-54.

37. Salam, M.T., et al., Mortality with brainstem seizures from focal 4-aminopyridine-induced recurrent hippocampal seizures. *Epilepsia*, 2017. 58(9): p. 1637-1644.
38. Kalume, F., et al., Sudden unexpected death in a mouse model of Dravet syndrome. *J Clin Invest*, 2013. 123(4): p. 1798-808.
39. Devinsky, O., et al., Sudden unexpected death in epilepsy: epidemiology, mechanisms, and prevention. *Lancet Neurol*, 2016. 15(10): p. 1075-88.
40. Lhatoo, S.D., et al., Nonseizure SUDEP: Sudden unexpected death in epilepsy without preceding epileptic seizures. *Epilepsia*, 2016. 57(7): p. 1161-8.
41. Devinsky, O., et al., Sudden unexpected death in epilepsy in patients treated with brain-responsive neurostimulation. *Epilepsia*, 2018. 59(3): p. 555-561.
42. Blumenfeld, H., et al., Cortical and subcortical networks in human secondarily generalized tonic-clonic seizures. *Brain*, 2009. 132(Pt 4): p. 999-1012.
43. Seneviratne, U., M. Cook, and W. D'Souza, The electroencephalogram of idiopathic generalized epilepsy. *Epilepsia*, 2012. 53(2): p. 234-48.
44. Naritoku, D.K., et al., Repetition of audiogenic seizures in genetically epilepsy-prone rats induces cortical epileptiform activity and additional seizure behaviors. *Exp Neurol*, 1992. 115(3): p. 317-24.
45. Jobe, P.C., et al., The genetically epilepsy-prone rat (GEPR). *Ital J Neurol Sci*, 1995. 16(1-2): p. 91-9.
46. Faingold, C.L., Brainstem Networks: Reticulo-Cortical Synchronization in Generalized Convulsive Seizures, in Jasper's Basic Mechanisms of the Epilepsies, J.L. Noebels, et al., *Editors*. 2012: Bethesda (MD).
47. Kreindler, A., et al., Electro-clinical features of convulsions induced by stimulation of brain stem. *J Neurophysiol*, 1958. 21(5): p. 430-6.
48. Browning, R.A. and D.K. Nelson, Modification of electroshock and pentylenetetrazol seizure patterns in rats after precollicular transections. *Exp Neurol*, 1986. 93(3): p. 546-56.
49. Merrill, M.A., et al., Brainstem seizure severity regulates forebrain seizure expression in the audiogenic kindling model. *Epilepsia*, 2005. 46(9): p. 1380-8.

SUPPLEMENTARY MATERIAL

FIGURE S1. Example of a non-fatal seizure associated with MUA and ECoG suppression in a freely behaving homozygous *Cacna1a*^{S218L} mouse.

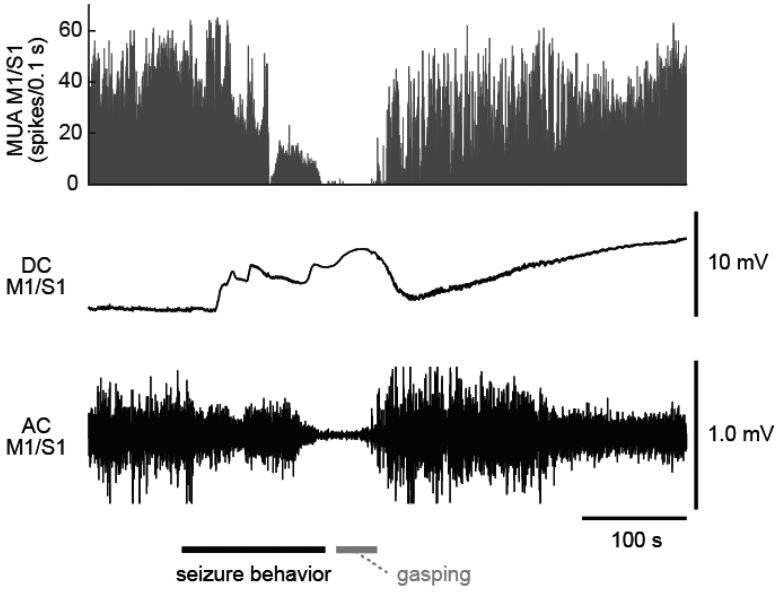

Late ictal and post-ictal suppression of cortical multi-unit activity (MUA) and ECoG lasted approximately 1 min. Local DC recording confirmed that suppression was not due to cortical spreading depolarization (SD), showing only movement-related DC-shifts during seizure behavior. Video recordings showed gasping behavior during recovery of MUA and ECoG activity, indicating successful autoresuscitation.

FIGURE S2. Cortical SD correlates with increased cortical DW-MRI signal intensity.

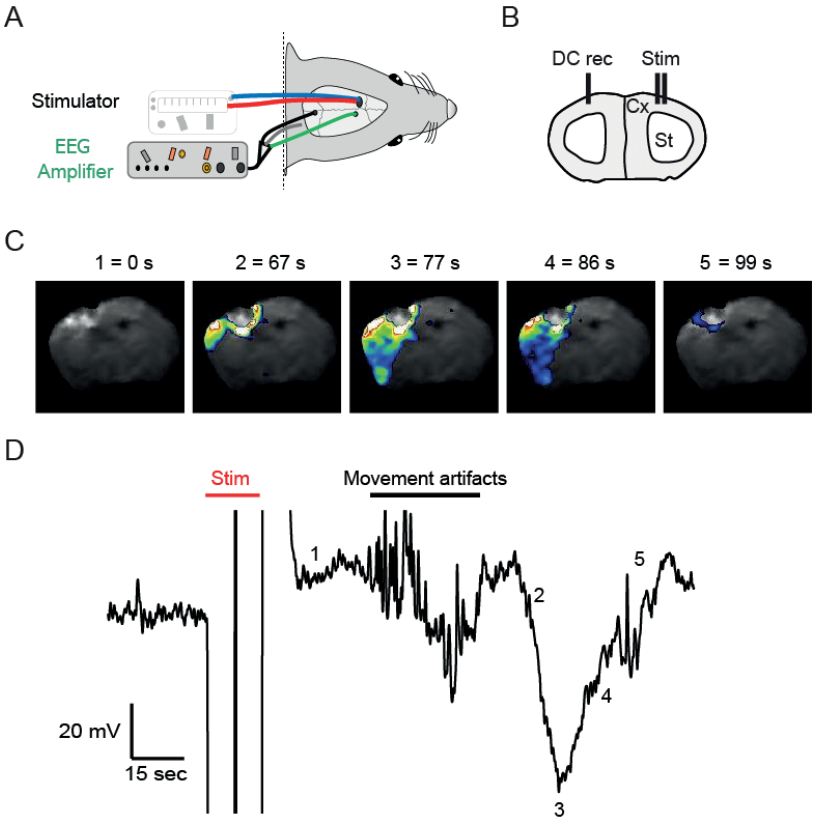

(A,B) Schematics showing placement of ECoG and stimulation electrodes in the contralateral cortex during simultaneous DW-MRI acquisition. **(C)** DW-MRI data showing spread of a single SD event, as measured by increased cell swelling, following seizure induction by electrical stimulation (Stim) of the cortex. Numbers denote the timing of the SD event as measured by DW-MRI relative to **(D)** the same SD event measured by ECoG. Note seizure-related movement artifacts prior to the cortical SD event. Cx = cortex; St = striatum.

FIGURE S3. Amygdala SD does not induce respiratory changes.

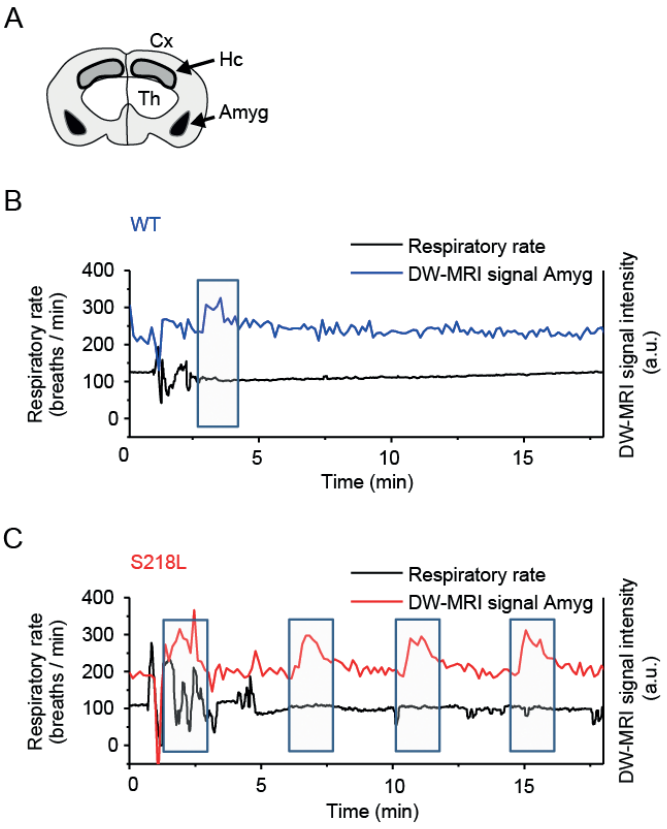

(A) Schematic map of coronal brain slice containing amygdala. **(B,C)** Representative traces of amygdala SD overlaid with respiratory rate for wild-type (WT) **(B)** and homozygous *Cacna1a*^{S218L} (S218L) **(C)** mice. SD events are outlined in blue rectangles. Note that for both the WT (panel B) and *Cacna1a*^{S218L} animal (panel C) SD is observed in the amygdala without any corresponding effect on respiration. A.u. = arbitrary units. Amyg = amygdala; Cx = cortex; Hc = hippocampus; Th = thalamus.